

Reduction kinetics of NiO–YSZ composite for application in solid oxide fuel cell

W. K. Yoshito · J. R. Matos · V. Ussui ·
D. R. R. Lazar · J. O. A. Paschoal

ICTAC2008 Conference
© Akadémiai Kiadó, Budapest, Hungary 2009

Abstract A porous nickel–8 mol% yttria stabilized zirconia (Ni–8YSZ) composite, used as anode for solid oxide fuel cell, was obtained by reduction of NiO–8YSZ cermet. The first goal was the evaluation of the temperature effect of powder processing by thermogravimetry. In addition, the influence of porosity in the reduction kinetic of the sample sintered at 1450 °C was evaluated. The final porosity produced in NiO–8YSZ composite by pore former was 30.4 and 37.9 vol.%, respectively, for 10 and 15 mass% of corn starch. The sample with 15 mass% of corn starch promotes a reduction rate almost twice higher than sample with 10 mass% of corn starch. The porosity introduced by the reduction of NiO was 23 vol.%.

Keywords Nickel oxide · Yttria stabilized zirconia · Coprecipitation · Thermal analysis · Reduction kinetic

Introduction

Nickel oxide–yttria stabilized zirconia (NiO–YSZ) composite is a material used most frequently as anode in the solid oxide fuel cell due to its high electrochemical activity for oxidation of hydrogen, high electrical conductivity, high thermodynamic stability and compatibility with other components of the cell [1].

The purpose of a large number of studies is to maximize the oxidation reaction. It is normally required that the anode materials present electronics percolation to allow the electron transport produced in the anode/electrolyte interface to the external current collector. They should also have enough porosity to transport the fuel to sites of triple phase boundary (TPB), among electrolyte, electrode and gas phase, and to transport the fuel oxidation products and vapors of water away from electrolyte/anode interface [1–3].

Usually the porous anode Ni–YSZ is made mainly of a mixture of powders of YSZ and NiO which is co-sintered with the electrolyte and cathode. The NiO is reduced to Ni⁰ “in situ” when the anode is exposed to fuel during cell operation. This procedure results in a significant change in mass, volume and the porosity of the composite, as well as their physical and mechanical properties.

It is known that the appropriate porosity of the anode is approximately 40% of the total volume of the composite. Considering that in the reduction of NiO to Ni⁰ about 41.1% of the initial volume of NiO is transferred to the pores, and that NiO concentration is around 54 mass%, the initial porosity of sintered NiO–YSZ composite should be between 10–20 vol.% [4].

In an X-ray diffraction study using the Rietveld refinement technique, Rojas et al. [5] observed that in the kinetic of reduction process, the volume of the unit cell of YSZ remains the same. Meanwhile, the volume of cell cubic structure of the nickel decreases with an increase in concentration of nickel in the composite.

Numerous studies reports that zirconia (ZrO₂) can be partly reduced at high temperature in reducing atmosphere. This reduction occurs usually above 500 °C and only on the surface [6, 7]. Dow et al. [8] presented a study where it is shown that the consumption of H₂ is approximately

W. K. Yoshito (✉) · V. Ussui · D. R. R. Lazar ·
J. O. A. Paschoal
Instituto de Pesquisas Energéticas e Nucleares, Av. Prof. Lineu
Prestes 2242, São Paulo, SP CEP 05508-000, Brazil
e-mail: wyoshito@ipen.br

J. R. Matos
Instituto de Química, Universidade de São Paulo, C.P. 26077,
São Paulo, SP 05513-970, Brazil

10×10^{-6} moles for 0.2 g of YSZ, confirming that YSZ is not easily reduced by H_2 .

The sintering of composites prepared from small sized powders ($<1 \mu\text{m}$) promote no formation of enough open porosity for percolation of gases through the anode. In this case, pores formers agents that decompose into gases during the heat treatment are usually added. Haslam et al. [9] presented a study of the influence of pore formers in the diffusion of H_2 gas in the reducing kinetics of the NiO to Ni^0 .

There are several methods for preparation of the Ni–YSZ composite as mechanical alloying [10], gel precipitation [11], combustion [12] and co-precipitation synthesis [13]. Among them co-precipitation is a large alternative in the manufacturing of the anode, because it allows a mixture of precursors already in the solution, resulting in a mixture of gel with a high degree of chemical homogeneity that ensures a uniform distribution of nickel particles in the ceramics matrix [14]. With regard to these comments, the purpose of this study is to evaluate the use of powders obtained by the co-precipitation technique, taking into account the effect of temperature in each stage of powders processing and finally the influence of porosity in the reduction kinetics of NiO to Ni^0 .

Experimental procedure

Zirconium oxychloride prepared from the caustic fusion of zircon sand (IPEN, Brazil), yttrium chloride (prepared by hydrochloric acid dissolution of 99,99% Y_2O_3 —Aldrich Chemical Co, USA and nickel chloride (obtained by aqueous dissolution of 98% nickel chloride hexahydrate—Merck) were the metallic ions precursors. Ammonium hydroxide (CAAL Brazil) was the precipitating agent.

The relative amounts of yttrium and zirconium were chosen to produce a final composition corresponding to 8 mol% yttria stabilized zirconia and the concentration of NiO was set for a final composition of the powders of NiO–YSZ with 56 mass% of NiO.

The coprecipitation reactions were carried out by spraying the mixed metal chlorides solution (heated at $95 \text{ }^\circ\text{C}$), into vigorously stirred ammonium hydroxide solution. The precipitates were filtered in vacuum and washed with distilled water to remove Cl^- ions. To avoid the formation of hard agglomerates the precipitates were washed with ethanol, followed by an azeotropic distillation with butanol. The resulting powders were oven-dried at $80 \text{ }^\circ\text{C}$ for 24 h, calcined at $800 \text{ }^\circ\text{C}$ for 1 h and milled in ethanol for 15 h using zirconia balls [15].

Powders were uniaxially pressed at 100 MPa as cylindrical pellets of 15 mm diameter and 1 mm height and sintered in air at $1450 \text{ }^\circ\text{C}$ for 1 h.

For the study of reduction kinetic influence of NiO on porosity, samples of NiO–YSZ were prepared with corn starch as pore former. The concentration of pore former was fixed at 10, 15 and 20 mass% of NiO in the composite. The powder was mixed in ethanol and oven dried at $80 \text{ }^\circ\text{C}$ and then deagglomerated in agate mortar. These samples were pressed using the same procedure used for the samples without pores formers.

In the sintering process it was maintained an isotherm of $600 \text{ }^\circ\text{C}$ for 30 min to ensure that all corn starch had been decomposed and removed from the sample and finally held in an isotherm of $1450 \text{ }^\circ\text{C}$ for 1 h. All sintering stages were performed in air.

TG/DTG data were obtained using Thermobalance TGA 51 model (Shimadzu), under dynamic air, N_2 and H_2/N_2 mixture atmospheres and heating rate of $10 \text{ }^\circ\text{C min}^{-1}$ to powders and $20 \text{ }^\circ\text{C min}^{-1}$ to ceramics. All experiments were performed in a platinum crucible.

Mass loss and thermal decomposition of the powders and corn starch was evaluated under heating up to $900 \text{ }^\circ\text{C}$, dynamic atmosphere of air at a total flow rate of 50 mL min^{-1} . The reduction kinetics of powders was carried out in dynamic 33% H_2/N_2 mixture atmosphere at a total flow rate of 100 mL min^{-1} .

The reduction kinetic studies of the ceramic bodies were performed in dynamic 50% H_2/N_2 mixture of atmosphere at a total flow rate of 100 mL min^{-1} , under heating up to $900 \text{ }^\circ\text{C}$ and holding isothermal in this temperature for 1 h.

Powders were characterized by X-ray diffraction (DMAX 2000, Rigaku) for crystal structure analysis, scanning electron microscopy (SEM) (XL30, Phillips) for particle and agglomerate morphology observation, transmission electron microscope (TEM) (200-C, JEOL) for the morphology and particle size evaluation, laser diffraction (granulometer 1064, Cilas) for agglomerate size distribution determination, N_2 gas absorption technique (BET) (Nova 1200, Quantachrome) for measurement of surface area and Helium pycnometry (Micromeritics, AccuPyc 1330) for density measurement.

The porosity of the samples after the reduction was determined by the immersion method described in ASTM C20-00 [16].

Results and discussion

Figure 1 shows the thermal decomposition of powders synthesized by co-precipitation. Two different stages were observed: dehydration and further decomposition to NiO–YSZ. The first mass loss event corresponds to the removal of free water molecules and organic solvents, occurs slowly and gradually between 25 and $280 \text{ }^\circ\text{C}$. The second event

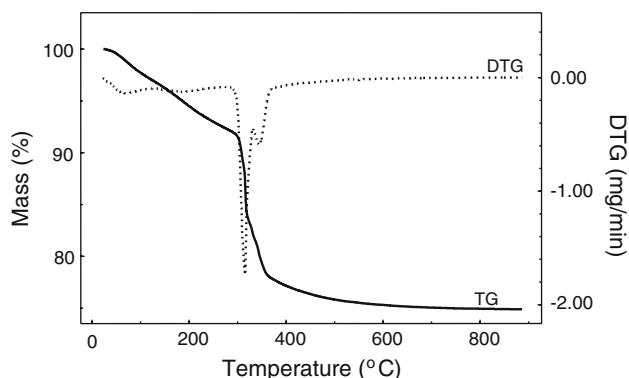


Fig. 1 TG/DTG curves of NiO–YSZ powders obtained by coprecipitation method obtained at 10 °C min⁻¹ under dynamic atmosphere of air (50 mL min⁻¹)

Table 1 Physical characteristics of NiO–YSZ powders obtained by co-precipitation

Agglomerate mean size (μm)	Specific surface area (m ² g ⁻¹)	Density (g cm ⁻³)	Crystallite size (nm)
0.3	23.2	6.00	20

that occurs in the 280–380 °C is associated to hydroxyl group linked to cations.

Table 1 presents results of agglomerate mean size, specific surface area, density and particle size of NiO–YSZ powder synthesized by co-precipitation route, calcined at 800 °C and milled for 15 h.

X-ray diffraction patterns of synthesized powders (Fig. 2) show the formation of a mixture of rhombohedral nickel oxide and tetragonal and/or cubic yttria stabilized zirconia.

The SEM micrograph in Fig. 3a shows that the NiO–YSZ powders are constituted of agglomerates of particles

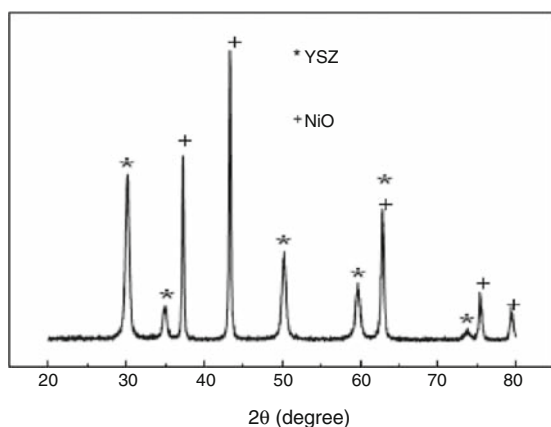


Fig. 2 XRD patterns of NiO–YSZ powders calcined at 800 °C for 1 h

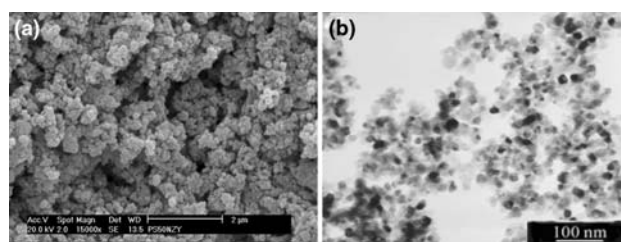


Fig. 3 SEM (a), and TEM (b) micrographs of NiO–YSZ powders synthesized by coprecipitation, calcined at 800 °C for 1 h and milled for 15 h

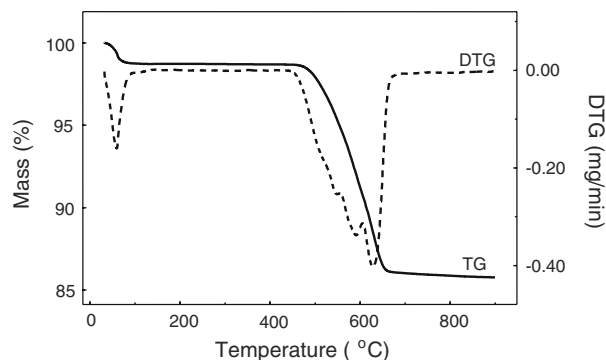


Fig. 4 TG/DTG curves obtained at 10 °C min⁻¹ under dynamic 33% H₂/N₂ mixture atmosphere (100 mL min⁻¹) for the reduction of NiO–YSZ powders

smaller than 1 μm. TEM micrograph (Fig. 3b) show particles near spherical shape and diameter of the 20 nm.

The TG/DTG curves illustrated in Fig. 4 show that the NiO–YSZ powders suffer no reduction until 465 °C. The first event (between 25 and 100 °C) is related to the elimination of water adsorbed on the surface of the powders. The second event that occurs between 460 and 660 °C is associated to reducing the NiO to Ni⁰. DTG curve indicates that the maximum rate of mass loss is due to the reduction that occurs at about 510 °C. The total mass loss in the second event is 12.7% corresponding to the reduction of stoichiometric NiO to Ni⁰, which agrees with the nominal concentration of NiO in the composite.

The TG/DTG curves of the NiO–YSZ composite sintered sample results presented in Fig. 5 indicate that the reduction begins at 460 °C. The reduction of NiO in NiO–YSZ composite occurs in two stages: the first stage is attributed to the removal of oxygen ions from the NiO, nucleation of Ni species and subsequent grain growth, which is very fast. The second stage is slower because NiO grains become less accessible, due to a metallic nickel layer that inhibits water removal.

The H₂ reduction of NiO occurs according to the following reaction [17]:

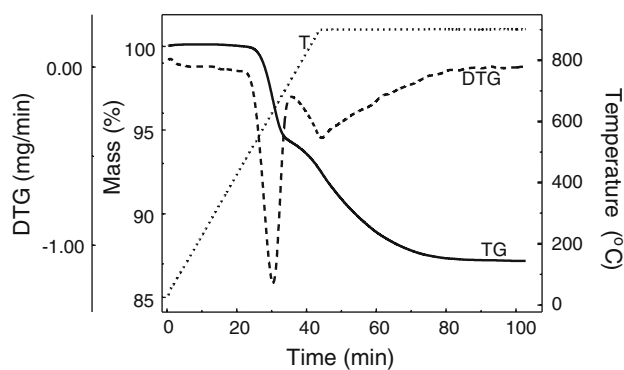


Fig. 5 TG/DTG and T curves of NiO–YSZ sintered sample obtained at $20\text{ }^{\circ}\text{C min}^{-1}$ under dynamic 50% H_2/N_2 mixture atmosphere (100 mL min^{-1}) and holding isothermal at $900\text{ }^{\circ}\text{C}$ for 1 h

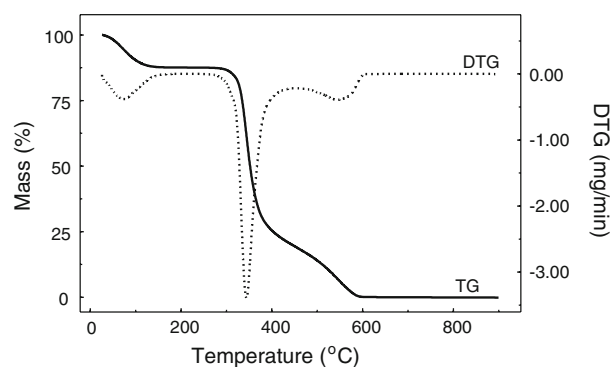
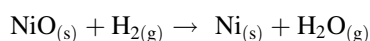


Fig. 6 TG/DTG curves of corn starch sample obtained at $20\text{ }^{\circ}\text{C min}^{-1}$ under dynamic air atmosphere (50 mL min^{-1})



DTG curve (Fig. 5) shows that the maximum reduction rate at $620\text{ }^{\circ}\text{C}$, and that the reduction process is completed in isotherm of $900\text{ }^{\circ}\text{C}$ after 57 min. During the NiO reduction process, the initial NiO volume is reduced by 41.1%, creating pores [4]. Despite this increase in the total amount of porosity the final value is not enough to fulfil the anode requirement. Literature indicates that the appropriate porosity level of Ni–YSZ cermet for anode application is around 40%. The procedure normally used to increase the porosity is to introduce pores formers such as graphite, corn starch or spherical polymers. Thus, the microstructure and pore structure are influenced by the size, shape and quantity of pores formers which, consequently will improve access to the active three-phase boundary region of the anode [18, 19].

The relative densities and porosity of the unreduced and reduced samples are presented in Table 2. The porosity introduced after reduction corresponds to the volume of NiO present in the original composition of the powders. Samples with 56 mass % of NiO has a porosity of 23% after the reduction.

Figure 6 shows typical TG/DTG curves for decomposition of corn starch (density 1.54 g cm^{-3}). It is observed that the thermal decomposition occur in two steps. The first mass loss, which is about 12% between 25 and $180\text{ }^{\circ}\text{C}$, is related to the elimination of water. The second step begins at $275\text{ }^{\circ}\text{C}$ due to decomposition of corn starch and is

Table 2 Apparent density values of NiO–YSZ and Ni–YSZ composites

Sample Code	Apparent density (g cm^{-3})	Relative density (%TD)	Porosity (%)
NiO–YSZ	6.35	95.8	0.79
Ni–YSZ	5.56	83.9	23.0

Table 3 Apparent density, relative density and porosity of sintered sample NiO–YSZ with different composition of corn starch

Sample code	Apparent density (g cm^{-3})	Relative density (% TD)	Porosity (%)
NiO–YSZ-CP10	5.53	83.4	6.92
NiO–YSZ-CP15	5.11	77.1	20.21
NiO–YSZ-CP20	4.78	72.1	26.46

associated to the thermal decomposition of carbohydrates with partial carbonization. The third step is the burning of the materials formed in the second step. The sample is completely decomposed at $600\text{ }^{\circ}\text{C}$ with the formation of gaseous products.

Table 3 shows the densities and porosity of the samples mixed with amounts of corn starch to produce ceramics bodies with a final composition corresponding to 10, 15 and 20 mass% of pore former. The samples were sintered in air at $1450\text{ }^{\circ}\text{C}$ for 1 h. In the studied samples the total porosity is between 6.92 and 26.46% from decomposition of corn starch. In this context the open porosity is appropriate to obtain a percolation of the porous phase after the reduction.

Figure 7 illustrates the TG/DTG curves of samples obtained from a thermal treatment of ceramics with 10, 15 and 20 mass% of pore former, respectively. It may be observed that the reduction rate is very fast at the beginning of the process. The DTG curve shows that the temperature where the maximum reduction takes place decreases with increasing amount of corn starch in the composition of the samples. The maximum reduction rate at temperatures of 596, 584 and $578\text{ }^{\circ}\text{C}$, for samples were obtained from 10, 15 and 20 mass% of corn starch, respectively.

To calculate the rate of reduction it was considered the onset and endset in the initial portion of the reduction curve. The reduction rate of sample with 20 mass% of corn starch was higher and reached 2.24 mg min^{-1} while the sample with 10 and 15 mass% of pores formers showed 1.64 and 1.61 mg min^{-1} , respectively.

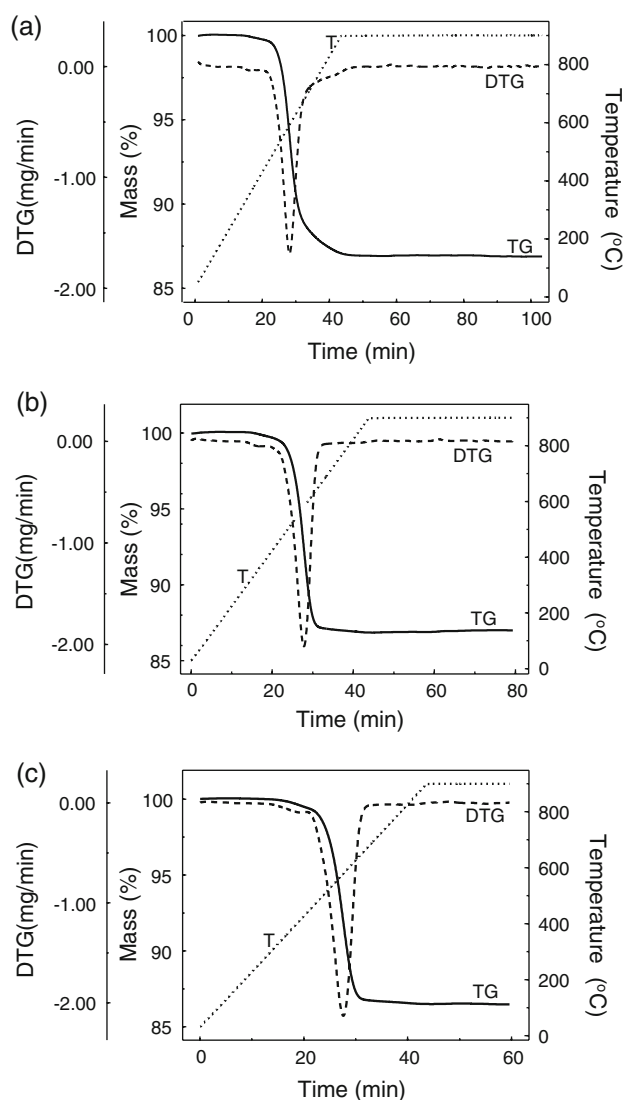


Fig. 7 TG/DTG and T curves obtained at $20\text{ }^{\circ}\text{C min}^{-1}$ under dynamic $50\% \text{H}_2/\text{N}_2$ mixture atmosphere (100 mL min^{-1}) and holding isothermal at $900\text{ }^{\circ}\text{C}$ for 1 h of NiO–YSZ sintered samples containing corn starch as pore former: **a** 10 mass%, **b** 15 mass% and **c** 20 mass%

This difference in the reduction rate is related to the larger surface area associated to the porosity of the composite, outer surface area and open pores. The high porosity favors the diffusion of $50\% \text{H}_2/\text{N}_2$ mixture gas. All the explanation above makes the consumption of H_2 by NiO extremely rapid, resulting in a shorter time of reduction.

As the reduction process begins in the both sides of the composite pellets, the reduction front advances toward the interior region and meet each other in the center of the sample. At this stage the reduction rate is controlled by diffusion of reducing mixture gas through the micropore generated by the reduction of NiO, and become slower. This behaviour causes a lower consumption of $50\% \text{H}_2/\text{N}_2$

Table 4 Density of sintered samples reduced under dynamic $50\% \text{H}_2/\text{N}_2$ mixture atmosphere at a total flow rate of 100 mL min^{-1} , and holding isothermal at $900\text{ }^{\circ}\text{C}$ during 1 h

Sample code	Apparent density (g cm^{-3})	Relative density (%TD)	Porosity (%)
NiO–YSZ-CP10	4.83	71.8	30.4
NiO–YSZ-CP15	4.43	67.3	37.9
NiO–YSZ-CP20	4.08	66.8	41.4

mixture gas thus a gradual decrease in the inclination of the curve of reduction is observed.

The larger porosity formation has a direct influence on the definition of onset temperature at which the reduction is shifted. For sample with 20 mass% of pore former the onset temperature of reduction is $690\text{ }^{\circ}\text{C}$, while for sample obtained with 15 mass% of pore former of the onset was $862\text{ }^{\circ}\text{C}$. The reduction of sample obtained with 10 mass% of corn starch was only completed after 5 min of dwell time in an isotherm of $900\text{ }^{\circ}\text{C}$.

In Table 4 values of apparent and relative density and porosity of the samples after the reduction are presented. Results indicate that for composition with 10 and 15 mass%, the final porosity reaches acceptable values [4].

Conclusions

The results show that the reduction of composites NiO–YSZ can be performed with dynamic $50\% \text{H}_2/\text{N}_2$ mixture atmosphere. The formation of a layer of Ni^0 on the NiO crystallites surface during the initial phase of the process of reduction inhibits water removal and the diffusion of reducing gas due to the decrease of the gas flow attributed to progressively generation of smaller pores. This factor normally prevents the complete reduction of the NiO–YSZ composite. As a consequence, the porosity produced by the reduction of nickel oxide was 23%, quite below the acceptable value to fulfil the anode requirement. Higher reduction rate was obtained by the incorporation of corn starch as pore former to NiO–YSZ.

Acknowledgements The authors wish to thank to Celso Vieira de Moraes, Nildemar Aparecido M. Ferreira, Ren  de Oliveira for their assistance in the characterization of NiO–YSZ composite, CNPq, FAPESP and CAPES.

References

- Dikwal CM, Bujalski W, Kendall K. The effect of temperature gradients on thermal cycling and isothermal ageing of micro-tubular solid oxide fuel cells. *J Power Sources*. 2008;193:241–8.
- Kawada T, Sakai N, Yokokawa H, Dokiya M, Mori M, Iwata T. Characteristics of slurry-coated nickel zirconia cermet anodes for solid oxide fuel cells. *Solid State Ionics*. 1990;137:3042–7.

3. Bieberle A, Méier LP, Gauckler LJ. The electrochemistry of Ni pattern anodes used as solid oxide fuel cell model electrodes. *J Electrochem Soc.* 2001;148:646–56.
4. Lee JH, Moon H, Lee HW, Kim J, Kim JD, Yoon KH. Quantitative analysis of microstructure and its related electrical property of SOFC anode, Ni–YSZ cermet. *Solid State Ionics.* 2002;148:15–26.
5. Rojas AR, Esparaza-Ponce HE, Fuentes L. In situ X-ray Rietveld analysis of Ni–YSZ solid oxide fuel cell anodes during NiO reduction in H₂. *J Phys D: Appl Phys.* 2005;38:2276–82.
6. Borer AL, Bronnimann C, Prins R. ZrO₂-promoted Rh/SiO₂ catalysts in CO hydrogenation and temperature-programmed reduction. *J Catal.* 1994;145:516–25.
7. Guglielminotti E, Giamello E, Pinna F, Strukul G, Martinengo S, Zanderighi L. Elementary steps in CO hydrogenation on Rh catalysts supported on ZrO₂ and Mo/ZrO₂. *J Catal.* 1994;146:422–36.
8. Dow WP, Wang YP, Huang TJ. Yttria-stabilized zirconia supported copper oxide catalyst I. Effect of oxygen vacancy of support on copper oxide. *J Catal.* 1996;160:155–70.
9. Haslam JJ, Pham AQ, Chung BW, DiCarlo JF, Glass RS. Effects of the use of pore formers on performance of an anode supported solid oxide fuel cell. *J Am Ceram Soc.* 2005;88:513–8.
10. Tietz F, Dias FJ, Simwonis D, Stover D. Evaluation of commercial nickel oxide powders for components in solid oxide fuel cells. *J Eur Ceram Soc.* 2000;20:1023–34.
11. Grgicak CM, Green RG, Du WF, Giorgi JB. SOFC anodes for direct oxidation of hydrogen and methane fuels containing H₂S. *J Am Ceram Soc.* 2005;88:3081–7.
12. Marinsek M, Zupan K, Maek J. Ni–YSZ cermet anodes prepared by citrate/nitrate combustion synthesis. *J Power Sources.* 2002;106:178–88.
13. Guo SLR, Li J, Chen Y, Liu W. Synthesis of NiO–ZrO₂ powders for solid oxide fuel cells. *Ceram Int.* 2003;29:883–6.
14. Yoshito WK, Ussui V, Lazar DRR, Paschoal JOA. Synthesis and characterization of NiO–8YSZ powders by co-precipitation route. *Mater Sci Forum.* 2005;498–499:612–7.
15. Ussui V, Leitão F, Yamagata C, Menezes CAB, Lazar DRR, Paschoal JOA. Synthesis of ZrO₂-based ceramics for applications in SOFC. *Mater Sci Forum.* 2003;416–418:681–6.
16. ASTM C20-00. Standard test methods for apparent porosity, water absorption, apparent specific gravity, and bulk density of burned refractory brick and shape by boiling water; 2005.
17. Wang Y, Walter ME, Sabolsky K, Seabaugh MM. Effects of powder sizes and reduction parameters on the strength of Ni–YSZ anodes. *Solid State Ionics.* 2006;177:1517–27.
18. Sanson A, Pinasco P, Roncari E. Influence of pore formers on slurry composition and microstructure of tape cast supporting anodes for SOFCs. *J Eur Ceram Soc.* 2008;28:1221–6.
19. Gregorová E, Pabst W, Bohacenko I. Characterization of different starch types for their application in ceramic processing. *J Eur Ceram Soc.* 2006;26:1301–9.